

1                   ***Streptococcus agalactiae* and *Escherichia coli* Induce Distinct Effector  $\gamma\delta$  T Cell**  
2                   **Responses During Neonatal Sepsis and Neuroinflammation**

3                   Lila T. Witt<sup>1,2</sup>, Kara G. Greenfield<sup>1</sup>, Kathryn A. Knoop<sup>1,3,\*</sup>

4                   <sup>1</sup> Department of Immunology, Mayo Clinic, Rochester MN, USA 55901

5                   <sup>2</sup> Mayo Graduate School of Biomedical Sciences, Mayo Clinic

6                   <sup>3</sup> Department of Pediatrics, Mayo Clinic

7                   Send correspondence to: [Knoop.Kathryn@mayo.edu](mailto:Knoop.Kathryn@mayo.edu)

8

9 **Abstract**

10 The neonatal phase of life is a time during which susceptibility to infection is particularly high, with  
11 prematurely born neonates being especially vulnerable to life-threatening conditions such as  
12 bacterial sepsis. While *Streptococcus agalactiae*, also known as group B *Streptococcus* (GBS)  
13 and *Escherichia coli* are frequent causative pathogens of neonatal sepsis, it is still unclear how  
14 the neonatal adaptive immune system responds to these pathogens. In the present study, we find  
15 that  $\gamma\delta$  T cells in neonatal mice rapidly respond to single-organism sepsis infections of GBS and  
16 *E. coli*, and that these infections induce distinct activation and effector functions from IFN- $\gamma$  and  
17 IL-17 producing  $\gamma\delta$  T cells, respectively. We also report differential reliance on  $\gamma\delta$ TCR signaling  
18 to elicit effector cytokine responses during neonatal sepsis, with IL-17 production during *E. coli*  
19 sepsis being associated with TCR signaling, whereas IFN- $\gamma$  production during GBS sepsis is  
20 TCR-independent. Furthermore, we report that the divergent effector responses of  $\gamma\delta$  during GBS  
21 and *E. coli* sepsis impart distinctive neuroinflammatory phenotypes on the neonatal brain. The  
22 present study sheds light on how the neonatal adaptive immune response responds differentially  
23 to bacterial stimuli and how these responses impact neonatal sepsis-associated  
24 neuroinflammation.

25 **Introduction**

26 Late-onset neonatal sepsis remains a leading cause of neonatal morbidity and mortality  
27 worldwide, particularly amongst preterm infants (Bergin et al., 2015; Stoll et al., 2011). The  
28 neonatal period, defined as the first 28 days of life in humans, is a time during which risk of  
29 infection is especially high, due in part to the relative immaturity of the neonatal immune system  
30 (Bergin et al., 2015; Knoop et al., 2020; Segura-Cervantes et al., 2016). Premature neonates are  
31 highly vulnerable to life-threatening conditions such as sepsis (Bizzarro et al., 2005; Dong and  
32 Speer, 2015; Wynn et al., 2015). Gram-negative bacilli such as *Klebsiella*, *Pseudomonas* and *E.*

33 *coli* are prevalent in the gastrointestinal tract of premature neonates and are capable of  
34 translocating from the gut and causing sepsis (Basu, 2015; Carl et al., 2014; Knoop et al., 2020).

35 Increased bacterial translocation from the neonatal gut is facilitated in part by selective  
36 deficiencies in gut barrier defense mechanisms, including decreased production of protective  
37 factors such as mucous, anti-microbial peptides, and IgA (Basu, 2015).

38 Conversely, Gram-positive neonatal sepsis is frequently caused by *Staphylococcus aureus* and  
39 *Streptococcus agalactiae*, or group B *Streptococcus* (GBS). GBS colonizes the neonate via  
40 vertical transmission during birth, often as the result of the neonate aspirating GBS-infected  
41 amniotic fluid (Heath and Jardine, 2014; Stoll et al., 2011). Although rates of GBS sepsis are  
42 declining due to improved early detection methods and prophylactic maternal antibiotic  
43 administration, the mortality rate of GBS sepsis can be as high as 10%, with 30-50% of survivors  
44 going on to experience neurological comorbidities in early childhood (Mynarek et al., 2021).

45 Although both GBS and *E. coli* can be found as components of a healthy microbiota, they have  
46 the potential to cause severe disease in vulnerable populations, such as neonates (Remington et  
47 al., 2010; Tavares et al., 2022). The increased risk of sepsis development amongst preterm  
48 neonates is further compounded by deficiencies in several innate immunological defense  
49 mechanisms, including decreased levels of circulating complement proteins, impaired neutrophil  
50 function, and reduced secretion of pro-inflammatory cytokines by dendritic cells compared to  
51 adults (Tsafaras et al., 2020). Similar to the innate immune system, the adaptive immune system  
52 in neonates bears several striking differences to that of adults (Tsafaras et al., 2020). Compared  
53 to adults, neonates have impaired memory T cell formation and are largely skewed toward Th2  
54 over Th1 differentiation, thereby impairing their ability to mount a proper immune response to  
55 microbial infections (Barrios et al., 1996; Basha et al., 2014; Li et al., 2004). Neonates also have  
56 deficiencies in humoral immunity, such as delayed germinal center formation and impaired  
57 antibody responses to both T cell dependent and independent antigens (Semmes et al., 2021)

58 Despite their relative impairments in the conventional T and B cell compartments, neonates have  
59 a significant population of  $\gamma\delta$  T cells (Basha et al., 2014).  $\gamma\delta$  T cells are innate-like lymphocytes  
60 that are abundant in barrier sites and act as early immune sentinels during infection (Chien et al.,  
61 2014; Vantourout and Hayday, 2013). In contrast to conventional CD4+ and CD8+ T cells,  $\gamma\delta$  T  
62 cells are exported from the thymus as functionally mature cells and are poised to rapidly deploy  
63 their effector functions upon the detection of microbial ligands or pro-inflammatory cytokines  
64 (Ribot et al., 2021). As the first T cells to develop in the embryonic thymus,  $\gamma\delta$  T cells are critical  
65 players in the neonatal immune response during a time when CD4+ and CD8+ T cells, and B cells  
66 are still developing and maturing (Dimova et al., 2015; Gibbons et al., 2009; Vantourout and  
67 Hayday, 2013). Indeed,  $\gamma\delta$  T cells have been found to play a critical role in host protection during  
68 neonatal influenza (Guo et al., 2018) and *Clostridium difficile* infection (Chen et al., 2020),  
69 underscoring their importance during early life.

70 In the present study, we characterize the immune responses to two major neonatal sepsis  
71 pathogens, *Streptococcus agalactiae* (Group B *Streptococcus*) and *Escherichia coli*. We report  
72 that these two pathogens induce distinct effector cytokine responses from gamma delta ( $\gamma\delta$ ) T  
73 cells in postnatal day 7 (P7) pups and that these responses differentially impact mortality. We  
74 also report that these two pathogens drive distinct neuroinflammatory phenotypes in neonatal  
75 mice. This study sheds light on how distinct sepsis pathogens drive differential adaptive immune  
76 responses in neonatal mice, impacting sepsis mortality and neuroinflammation.

## 77 **Results**

### 78 *$\gamma\delta$ T cells Respond to E. coli and GBS Neonatal Sepsis and Differentially Drive Mortality*

79 While group B *Streptococcus* (GBS) and *Escherichia coli* are frequent causative pathogens of  
80 neonatal sepsis, it is still unclear how features of these bacteria differentially drive the neonatal  
81 adaptive immune response (Tsai et al., 2014). Therefore, we infected C57BL/6 P7 mice with a

82 single-organism infection of either  $10^6$  CFU *Streptococcus agalactiae* (GBS) or  $2 \times 10^4$  CFU *E. coli*.  
83 Both *E. coli* and GBS septicemia induced robust activation from  $\gamma\delta$  T cells in the spleen 18 hours  
84 post-infection, as measured by an increase the proportion of CD69+ CD62L-  $\gamma\delta$  T cells compared  
85 to uninfected controls (Fig. 1a). A modest increase in the activation status of conventional CD4+  
86 and CD8+ T cells, and B cells was also observed (Fig. S1a-c). Paralleling clinical findings, P7  
87 mice infected with Gram-negative *E. coli* experienced decreased survival compared to Gram-  
88 positive GBS (Tsai et al., 2014), despite the higher bacterial burden in GBS-infected pups at 18  
89 hours post-infection (Fig. 1b-d). Similarly, greater  $\gamma\delta$  T cell activation was also observed in *E. coli*  
90 compared to GBS-infected pups (Fig. 1a). Interestingly, antibody-mediated depletion of  $\gamma\delta$  T  
91 cells in *E. coli* infected mice was sufficient to completely rescue mortality (Fig. 1c), however no  
92 differences in survival were observed in GBS- infected pups upon depletion of  $\gamma\delta$  T cells (Fig. 1b).  
93 Of note, depleting  $\gamma\delta$  T cells did not impact either GBS or *E. coli* bacterial burden in neonatal pups  
94 (Fig. 1d), suggesting that  $\gamma\delta$  T cells do not impact anti-microbial immune defenses during  
95 neonatal sepsis. These data indicate that although  $\gamma\delta$  T cells undergo activation during both GBS  
96 and *E. coli* neonatal sepsis infection, those responses differentially impact mortality independent  
97 of systemic bacterial burden.

98 *E. coli* and GBS Neonatal Sepsis Drive Distinct Effector Cytokine Responses from  $\gamma\delta$  T cells

99 Due to the differential impact of  $\gamma\delta$  T cells on mortality during GBS vs. *E. coli* neonatal sepsis, we  
100 next sought to further characterize the responses of  $\gamma\delta$  T cells during these two single-organism  
101 sepsis infections.  $\gamma\delta$  T cells undergo developmental programming in the thymus and exist in the  
102 periphery as either those that produce either IL-17 or IFN- $\gamma$  (Haas et al., 2009; Muñoz-Ruiz et al.,  
103 2017; Ribot et al., 2009). These distinct effector programs can also be discerned based on the  
104 expression of certain surface markers, such as CCR6, restricted to IL-17 producing  $\gamma\delta$  T cells,  
105 and CD27, restricted to IFN- $\gamma$  producing  $\gamma\delta$  T cells (Ribot et al., 2009). We therefore asked if  
106 different subsets of  $\gamma\delta$  T cells were being activated during GBS and *E. coli* infection in neonates.

107 Cytokine staining of  $\gamma\delta$  T cells revealed a robust increase in IL-17 expression during *E. coli*, but  
108 not GBS infection whereas GBS induced increased IFN- $\gamma$ , but not IL-17, expression from  $\gamma\delta$  T  
109 cells (Fig. 2a-c). These findings were validated with serum ELISA, showing systemic increases in  
110 these cytokines during GBS and *E. coli* sepsis infections (Fig. 2d,e). Accordingly,  $\gamma\delta$  T cell  
111 activation during GBS infection was restricted to those expressing CD27, whereas during *E. coli*  
112 infection,  $\gamma\delta$  T cell activation was restricted to the CCR6+ expressing fraction (Fig. 2f,g),  
113 suggesting GBS and *E. coli* infections induce discrete activation of  $\gamma\delta$  T cell subsets. Therefore,  
114 single-organism GBS and *E. coli* infections in neonates induces specific activation of different  $\gamma\delta$   
115 T cell populations, resulting in distinct effector cytokine profiles.

116 *Neuroinflammation is a Feature of *E. coli* and GBS Neonatal Sepsis*

117 Adverse neurologic outcomes are associated with inflammatory events in early life (Mynarek et  
118 al., 2021; Stoll et al., 2004) however, how the adaptive immune response contributes to these  
119 outcomes remains poorly understood. Both *E. coli* and GBS were present in the brains of P7 pups  
120 18 hours post-infection, with increased CFUs of GBS present compared to *E. coli* (Fig. 3a). Flow  
121 cytometry analysis of CD45<sup>hi</sup> immune cells in the perfused brains of P7 pups revealed a significant  
122 increase in monocytes and neutrophils in the brains of *E. coli* infected pups compared to  
123 uninfected and GBS-infected pups (Fig. 3b,c). Interestingly, no significant increase in brain-  
124 infiltrating monocytes or neutrophils was noted in GBS-infected pups compared to control mice,  
125 despite the presence of GBS in the brain (Fig. 3b,c). To further investigate the neuroinflammatory  
126 phenotype associated with GBS and *E. coli* sepsis infection in neonates, we measured mRNA of  
127 immunological genes from bulk brain tissue on the Nanostring nCounter Gene Expression  
128 platform. In the brains of both GBS and *E. coli* infected P7 pups, there was a significant increase  
129 in the expression of monocyte and neutrophil chemotactic factors, such as *Ccl2* and *Cxcl1*,  
130 respectively (Fig. 3d,e). Compared to uninfected pups, the brains of GBS-infected pups had  
131 increased expression of genes involved in the innate immune response to Gram-positive bacteria,

132 such as *Tlr1* and *Tlr2* (Fig. 3d). *E. coli* brains had increased expression of genes associated with  
133 TLR4 activation, such as *Cd14*, and the complement pathway, such as *C3* and *Marco* (Fig. 3e).  
134 There were twenty-four differentially expressed genes between the brains of GBS and *E. coli*  
135 infected mice including increased expression of *casp-3* during GBS infection, and increased *Il23*  
136 expression during *E. coli* infection (Fig. 3e). These findings indicate that although both GBS and  
137 *E. coli* can cause neuroinflammation during single-organism neonatal sepsis infection, they  
138 induce distinct inflammatory phenotypes.

139 *TCR-Specific Activation of  $\gamma\delta$  T cells Occurs During *E. coli*, but not GBS, Septicemia and Sepsis-*  
140 *Associated Neuroinflammation*

141  $\gamma\delta$  T cells are capable of undergoing activation via multiple pathways, including MHC-independent  
142 TCR activation by pathogen-derived non-peptide antigens (Constant et al., 1994). Nur77 is  
143 transcription factor that is rapidly and specifically expressed during antigen-receptor mediated  
144 signaling and activation in T and B cells (Ashouri and Weiss, 2017; Moran et al., 2011). Therefore,  
145 to determine if  $\gamma\delta$ TCR signaling was occurring in GBS and *E. coli* sepsis infection in mice, we  
146 utilized P7 Nur77-GFP reporter pups. In the spleens of *E. coli* infected P7 pups, there was an  
147 increase in the proportion of Nur77+ CD69+  $\gamma\delta$  T cells (Fig. 4a), indicating TCR-mediated  
148 activation of  $\gamma\delta$  T cells was occurring during *E. coli* neonatal sepsis infection. Importantly, nearly  
149 all of these Nur77+ CD69+ cells in the spleen are CCR6+ (Fig. 4c), suggesting that the IL-17  
150 signature during *E. coli* neonatal sepsis is associated with TCR signaling. Interestingly, there was  
151 no change in the proportion of Nur77+ CD69+  $\gamma\delta$  T cells in the spleens of GBS infected pups (Fig.  
152 4a). These data suggest that during GBS infection, CD27+  $\gamma\delta$  T cells undergo TCR-independent  
153 activation. These data suggest that the CCR6+  $\gamma\delta$  T cells responding to *E. coli* and CD27+  $\gamma\delta$  T  
154 cells responding to GBS neonatal sepsis undergo distinct pathways of activation to elicit their  
155 effector cytokine responses.

156  $\gamma\delta$  T cells play an important role in CNS homeostasis (Park et al., 2022; Ribeiro et al., 2019a) and  
157 have been shown to have both a protective (Gentles et al., 2015) and detrimental (Gelderblom et  
158 al., 2014; Welte et al., 2008) effect on the CNS under inflammatory conditions. We therefore  
159 hypothesized that distinct  $\gamma\delta$  T cell responses in the periphery during GBS and *E. coli* sepsis  
160 would impart a differential role for  $\gamma\delta$  T cells during sepsis-associated neuroinflammation.  $\gamma\delta$  T  
161 cells within the CNS are highly skewed toward IL-17 production and CCR6 expression (Ribeiro et  
162 al., 2019b; Wo et al., 2020). Similar to the spleen, we observed an increase in the proportion of  
163 Nur77+ CD69+  $\gamma\delta$  T cells in the brains of *E. coli*, but not GBS infected mice (Fig. 4b), with the  
164 majority of Nur77+ CD69+  $\gamma\delta$  T cells expressing CCR6 (Fig. 4c), suggesting that in the brain,  
165 there is  $\gamma\delta$ TCR specific signaling of IL-17 producing  $\gamma\delta$  T cells.

166  *$\gamma\delta$  T cell Responses During *E. coli* and GBS Septicemia Differentially Impact Sepsis-Associated  
167 Neuroinflammation*

168 In order to determine the contribution of  $\gamma\delta$  T cells to GBS and *E. coli* sepsis-associated  
169 neuroinflammation, we compared immunological gene expression between BL/6 and TCR $\delta$ /-  
170 infected pups. TCR $\delta$ /- were used in this instance due to the lack of depletion of brain-resident  $\gamma\delta$   
171 T cells during anti-TCR $\gamma\delta$  antibody administration (Fig. S3a, b). Analysis of the brain by  
172 Nanostring revealed sixty differentially expressed genes between BL/6 and TCR $\delta$ /- *E. coli*  
173 infected pups, and twenty-four differentially expressed genes between BL/6 and TCR $\delta$ /- GBS  
174 infected pups. Compared to BL/6 *E. coli* infected pups, TCR $\delta$ /- pups had increased expression  
175 of genes associated with apoptosis, such as *Casp-3*, and *Mapk1* (Fig. 4d). These findings  
176 suggesting that during *E. coli* neonatal sepsis,  $\gamma\delta$  T cells may protect the neonatal brain from  
177 inflammation-induced cell death. Compared to BL/6 GBS-infected mice, TCR $\delta$ /- GBS infected  
178 pups had decreased expression of genes involved in antigen presentation, such as *H2-Dmb2* and  
179 genes involved in TGF- $\beta$  signaling, such as *Tgfb1* and *Smad5* (Fig. 4e). Genes involved in  
180 apoptosis, such as *Casp-3*, were not significantly differentially expressed between TCR $\delta$ /- and

181 BL/6 GBS infected pups, though it was increased in BL/6 GBS infected pups compared to BL/6  
182 *E. coli* infected pups (Fig. 4e). Taken together, these data suggest that  $\gamma\delta$  T cells play a context-  
183 specific role during sepsis-associated neuroinflammation.

184 **Discussion**

185 The present study reveals that  $\gamma\delta$  T cells undergo rapid activation and cytokine production during  
186 a murine model of single-organism *Streptococcus agalactiae* (GBS) and *Escherichia coli* neonatal  
187 sepsis infection. We also report that GBS and *E. coli* septicemia induce specific activation of IFN-  
188  $\gamma$  and IL-17 producing  $\gamma\delta$  T cells, respectively (Fig. 2). Although the  $\gamma\delta$  T cell compartment had  
189 the highest proportion of cells undergoing activation in response to both *E. coli* and GBS sepsis  
190 infections, a modest increase in activation status was observed for CD4+ and CD8+ T cells (Fig.  
191 S1). This small proportion of activated CD4 and CD8 T cells may represent “virtual memory” ( $T_{VM}$ )  
192 T cells, which are abundant in neonates (Akue et al., 2012; Schüler et al., 2004). Increased  
193 activation status of CD4+ and CD8+ T cells at the early timepoint of 18 hours post-infection may  
194 further implicate  $T_{VM}$  cells, as they are capable of responding to infection faster naïve T cells due  
195 to their memory-like capacity (Haluszczak et al., 2009; Lee et al., 2013).

196 In the context of *E. coli* infection, the presence of  $\gamma\delta$  T cells was found to be detrimental to the  
197 survival of neonatal mice, whereas the presence of  $\gamma\delta$  T cells had no effect on survival of neonatal  
198 pups during GBS infection (Fig. 1b, c). Furthermore, improved survival of pups in the absence of  
199  $\gamma\delta$  T cells during *E. coli* sepsis infection may be directly due to IL-17, the neutralization of which  
200 has been shown to improve sepsis survival outcomes in other models of neonatal sepsis (Wynn  
201 et al., 2016). This contrasts with other infections, such as neonatal murine influenza, in which  
202 neonatal mice lacking  $\gamma\delta$  T cells rapidly succumbed to infection (Guo et al., 2018). The apparent  
203 contradictory role of  $\gamma\delta$  T cells as pathogenic during sepsis vs. protective during other neonatal

204 infections could be due to the state of immune dysregulation and hyperinflammation that occurs  
205 during sepsis.

206 Despite greater bacterial burden in the GBS sepsis infection,  $\gamma\delta$  T cells were more activated in  
207 the context of *E. coli* sepsis infection (Fig. 1a,d), suggesting that specific bacterial factors, not just  
208 bacterial burden, are more important in dictating the magnitude of a the neonatal  $\gamma\delta$  T cell  
209 response. An additional outstanding question raised from this study is the extent to which  $\gamma\delta$   
210 cytokine responses depend directly on bacterial factors vs. the upstream immune response to  
211 those bacterial factors, and whether  $\gamma\delta$  T cells are more likely to produce a certain cytokine in  
212 response to specific virulence factors expressed by the bacteria. The clinical isolate of *E. coli*  
213 used herein is an extraintestinal pathogenic *E. coli* (ExPEC) that expresses a number of virulence  
214 genes, including the capsular polysaccharide K1 (Carl et al., 2014; Knoop et al., 2020). The K1  
215 antigen has been implicated in various neonatal infections, including meningitis and sepsis  
216 (Kaczmarek et al., 2014) and plays a critical role in the ability of *E. coli* to resist phagocytosis and  
217 invade the central nervous system (Hoffman et al., 1999). Similarly, GBS COH-1 (ATCC) is a  
218 highly virulent, encapsulated serotype III clinical isolate that expresses several virulence genes  
219 involved in immune resistance and neuroinvasion. Included amongst these virulence factors is  
220 the serine protease *CspA*, which has been implicated in the ability of GBS COH-1 to evade  
221 opsonophagocytosis (Harris et al., 2003). GBS is also highly neuroinvasive and represents a  
222 major causative pathogen of neonatal meningitis (Tavares et al., 2022). GBS COH-1 expresses  
223 invasion associated gene (*lsgA*), which has been implicated in the ability of GBS to infect human  
224 brain microvascular endothelial cells (Doran et al., 2005). Furthermore, the extent to which  
225 individual virulence factors expressed by *E. coli* and GBS induce specific  $\gamma\delta$  T cell activation  
226 requires further investigation.

227 We also report that during *E. coli* and GBS sepsis infection,  $\gamma\delta$  T cells undergo distinct pathways  
228 of activation in order to elicit their effector cytokine responses. While TCR-mediated activation

229 was associated with the production of IL-17 by  $\gamma\delta$  T cells during *E. coli* infection, we observed a  
230 lack of Nur77 induction that during GBS infection, suggesting that  $\gamma\delta$  T cells likely use a TCR-  
231 independent mechanism to undergo activation and produce IFN- $\gamma$  (Fig. 4a). Similar to NK cells,  
232  $\gamma\delta$  T cells can produce IFN- $\gamma$  in response to cytokines, such as IL-12, and IL-18 (Silva-Santos et  
233 al., 2019), and in response to NKG2D ligands (Sedlak et al., 2014). Furthermore, the exact  
234 mechanism by which CD27+  $\gamma\delta$  T cells become activated and make IFN- $\gamma$  during GBS infection  
235 will be the subject of future studies.

236 In addition to the danger that sepsis poses to infants in the short-term, there are also several long-  
237 term consequences that are common in survivors of neonatal sepsis. Poor neurological  
238 outcomes, such as impaired neurologic growth, and the development of cerebral palsy, have been  
239 associated with early life inflammatory events, including sepsis (Stoll et al., 2004). Although  
240 mechanisms by which early life inflammation contributes to this phenomenon remain under  
241 investigation, it is thought that inflammatory factors disrupt neuronal connectivity in the developing  
242 brain (Cardoso et al., 2015). While both GBS and *E. coli* can cause severe neuroinflammation in  
243 neonates (Kim, 2006; Tavares et al., 2022) how the neonatal adaptive immune response impacts  
244 sepsis-associated neuroinflammation remains poorly understood. The present study therefore  
245 sought to characterize the unique neuroinflammatory signatures associated with GBS and *E. coli*  
246 systemic infection, and the extent to which these signatures are dependent upon  $\gamma\delta$  T cells. Both  
247 GBS and *E. coli* were found in the brains of infected P7 pups, with slightly higher CFUs of GBS  
248 compared to *E. coli*, similar to the periphery (Fig. 4a compared to 1d). *E. coli* infection also induced  
249 greater infiltration of monocytes and neutrophils in the brain (Fig. 3b,c) despite both GBS and *E.*  
250 *coli* showing increased gene expression of *Cxcl1* and *Cxcl10* (Fig. 3d,e). Therefore, this  
251 recruitment may instead be due to the expression of bacterial factors, specific to *E. coli*, that act  
252 as a direct chemotactic signal for these cells. Increased *casp-3* expression was observed in the  
253 brains of *E. coli* infected TCR $\delta$ -/- pups compared to WT infected pups, suggesting that the  $\gamma\delta$  T

254 cell response in the brain during *E. coli* infection helps to prevent inflammation-induced cell death  
255 in the developing brain (Fig. 4d). Interestingly, no significant increase in *casp-3* expression was  
256 observed in GBS infected TCR $\delta$ -/- pups compared to WT infected pups (Fig. 3f). These data may  
257 suggest that the specific  $\gamma\delta$  T cell responses during *E. coli* infection, possibly by IL-17 production,  
258 promote cell survival in the developing brain. IL-17 has been shown to have an antiapoptotic effect  
259 on tumor cells (Nam et al., 2008), and to help promote the survival of B cells and their  
260 differentiation into plasma cells (Xu and Cao, 2010), but its specific role in this context remains  
261 unknown. Furthermore, whether the induction of *Casp-3* and cell death in the brain is protective  
262 or pathogenic requires further study.

263 During neonatal GBS infection, there was decreased expression of the *H2-Dmb2* gene in the  
264 absence of  $\gamma\delta$  T cells. H2-Dmb2 is involved in the removal of CLIP from MHC class II molecules  
265 and is critical for proper antigen presentation (Doebele et al., 2000; Santambrogio et al., 2019).  
266 Although it is well-known that IFN- $\gamma$  induces MHC II presentation (Kambayashi and Laufer, 2014;  
267 Wijdeven et al., 2018), whether the decreased expression of molecules associated with MHC II  
268 expression is dependent upon  $\gamma\delta$  T cell-derived IFN- $\gamma$  during GBS infection also requires further  
269 study. Similarly, *Il6ra*, *Tgfb1*, and *Smad3* were also increased in the BL/6 compared to TCR $\delta$ -/-  
270 GBS infected pups, suggesting that during GBS infection,  $\gamma\delta$  T cells may impact TGF- $\beta$  signaling.  
271 Overall, these findings present evidence of context-specific  $\gamma\delta$  T cell responses during neonatal  
272 sepsis, with these responses differentially impacting survival and neuroinflammation. Taken  
273 together, we report that  $\gamma\delta$  T cell responses during neonatal sepsis rely heavily on the initiating  
274 pathogen. This work will help elucidate the contributions of neonatal  $\gamma\delta$  T cells to sepsis induced  
275 mortality and neuroinflammation.

276

277 **Methods**

278 *Bacteria*

279 Clinical *E. coli* isolates were prepared as described previously (Knoop et al., 2020). GBS COH-1  
280 was obtained from ATCC. Single bacterial colonies of GBS and *E. coli* were taken from a streak  
281 plate and placed in a 15 mL conical (Fisher Healthcare) containing 5 mL of LB broth (Fisher  
282 Healthcare) and placed into a 37°C incubator overnight. The following day, 10 mL of LB broth was  
283 measured into a 50 mL conical tube (Fisher Healthcare) and a sterile dropper was used to place  
284 2-3 drops of overnight bacterial stock into fresh LB broth. Bacteria was shaken at 150 rpm at 37°C  
285 until an OD of 0.3 was reached. The bacterial culture was spun down at 12000 rpm for 10 minutes  
286 (*E. coli*) or 30 minutes (GBS) and the LB supernatant was discarded. The bacterial pellet was  
287 resuspended in 10mL of sterile PBS (Life Technologies) and a dose of 2x10<sup>4</sup> CFU (*E. coli*) or 10<sup>6</sup>  
288 CFU (GBS) was intraperitoneally injected into the neonatal pups with an insulin syringe (Cardinal  
289 Healthcare).

290 *Mice*

291 C57BL/6, TCRδ<sup>-/-</sup> and Nur77-GFP mice were purchased from Jackson Laboratory. All animals  
292 were bred in accordance with the Institutional Animal Care and Use Committee at Mayo Clinic.  
293 Anti-TCRγδ antibody (UC7-13D5, Biolegend) was given intraperitoneally for *in vivo* depletion of  
294 γδ T cells (15 µg/g body weight).

295 *Infection Model*

296 Neonatal mice were infected on postnatal day 7 (P7). Spleens were harvested 18 hours post-  
297 infection and blood was collected and allowed to clot for 45 minutes at room temperature and  
298 spun down at 10,000xg for 2 minutes. Serum was collected and was stored at -20°C until use.  
299 The liver was digested in 1mL of sterile PBS (Life Technologies) and 0.5 g of zirconium beads  
300 (Fisher Healthcare) in a safe-lock snap cap tube (Fisher Healthcare) and placed into a tissue  
301 homogenizer for 5 minutes. The liver homogenate was then serially diluted in PBS to achieve a

302 1:10<sup>5</sup> dilution (*E. coli*) and 1:10<sup>6</sup> dilution (GBS). Bacterial homogenate from *E. coli* and GBS  
303 infected pups was plated on either MacConkey agar plates (Fisher Healthcare) or Tryptic Soy  
304 Agar (DIFCO) respectively and CFUs were counted the following day.

305 *ELISA*

306 The following mouse ELISA kits were used: IL-17 DuoSet (Fisher Healthcare), IFN- $\gamma$  ELISAmax  
307 (Biolegend), ELISAs were performed according to manufacturer's instructions. Serum samples  
308 were diluted 1:5 in ELISA diluent buffer (Biolegend).

309 *Flow Cytometry*

310 Spleens were harvested from mice and were placed in 1 mL of RPMI 1640 (VWR International  
311 LLC), spleens were then mechanically homogenized using the frosted end of two glass slides  
312 (Fisher Healthcare). Spleens were counted using a hemocytometer. Cells were then spun down  
313 and resuspended in 500  $\mu$ L FACS buffer (PBS containing 5% human serum, 0.5% BSA, 0.1%  
314 sodium azide) and allowed to block for 20 minutes at 4°C. Surface master mix was made in FACS  
315 buffer and staining was performed for 30 minutes in the dark at 4°C. Following this staining,  
316 samples were washed twice with FACS buffer and samples were acquired on the CyTek Northern  
317 Lights Spectral Flow Cytometer (Cytek Biosciences).

318 *Intracellular cytokine staining*

319 Cells were placed in 250  $\mu$ L RPMI supplemented with 10% FBS, 2mM Glutamine (Gibco), 2mM  
320 Pyruvate (BioWhittaker), 50  $\mu$ g/mL Pen/Strep (BioWhittaker), and 0.55 mM 2-ME (Gibco). 1X  
321 protein transport inhibitor (Fisher Healthcare) and 1:1000 PMA/Ionomycin (Biolegend) were  
322 added, and samples were placed in an incubator at 37°C for four hours. Samples were spun down  
323 and resuspended in FACS buffer to block for 15 minutes. Samples were then stained for surface  
324 markers for 30 minutes at 4°C before 100  $\mu$ L of fixative (Life Technologies) was added to each

325 sample for 30 minutes at room temperature. Samples were then washed once with FACS buffer  
326 and once with 1X perm buffer (Biolegend) and spun down at 1500 rpm for 5 minutes. Samples  
327 were then resuspended in 100  $\mu$ L 1X perm buffer and intracellular antibodies and were placed at  
328 4°C overnight. The following day, samples were washed twice with FACS buffer and acquired on  
329 the CyTek Northern Lights Spectral Flow Cytometer.

330

331

332 The following antibodies were used for flow cytometry analysis:

Target	Fluorophore	Clone	Vendor	Titration
CD45	PE/Cy7, BV605	30-F11	Biolegend	1:500
CD4	BV421	GK1.5	Biolegend	1:500
CD8	BV510	53-6.7	Biolegend	1:250
CD11b	BV510	M1/70	Biolegend	1:250
TCRgd	BV421, PE	GL3	Biolegend	1:250
Viability	Zombie NIR, Violet	N/A	Biolegend	1:1000
Ly6G	APC	1A8	Biolegend	1:250
CD69	FITC, BV650	H1.2F3	Biolegend	1:250
CD62L	PE/Cy5	MEL-14	Biolegend	1:250
CCR6	BV785, APC	29-2L17	Biolegend	1:250
CD27	BV421	LG.3A10	Biolegend	1:250
Ly6C	PerCP	HK1.4	Biolegend	1:250
IL-17A	APC, PE	TC-11-18H10.1	Biolegend	1:100
IFN-g	PE, FITC	XMG1.2	BD Biosciences	1:100
TCR $\beta$	BV711	H57-597	Biolegend	1:250
CD19	APC/Cy7	6D5	Biolegend	1:250
CD3	APC/Cy7	17A2	Biolegend	1:250

333 *Brain Isolation for Analysis by Flow Cytometry*

334 Mice were anesthetized with 10 ug/g of Ketamine/Xyalizine mixture and transcardially perfused  
335 with 10 mL of cold, sterile PBS (Life Technologies). Brains were digested as previously described  
336 (Cumba Garcia et al., 2016). In brief, brains were isolated and placed into a 50 mL conical tube  
337 (Fisher Healthcare) containing 5 mL of RPMI (VWR International LLC). The RPMI containing the  
338 brains of the mice were then transferred to a 7 mL glass Tenbroeck dounce homogenizer (Pyrex)  
339 and homogenized until the brain was visibly digested (about 10 plunges). The homogenate was  
340 then poured through a 70  $\mu$ m filter into a new 50 mL conical tube, and 10 more mL of RPMI 1640  
341 was added, along with 1 mL of 10X PBS and 9 mL of Percoll (Sigma-Aldrich INC). The 50 mL  
342 conical tubes were then placed into a centrifuge and pelleted at 7840xg for 30 minutes at 4°C.  
343 Following the spin, the supernatant was fully aspirated off and samples were washed with 50 mL  
344 of fresh RPMI 1640 and spun again at 1500 rpm for 10 minutes. Samples were then blocked in  
345 FACS buffer for 15 minutes before surface staining was performed at 4°C for 30 minutes.

346 *mRNA Isolation from Brains* Brains were homogenized in 1 mL of sterile PBS (Life Technologies)  
347 using a dounce homogenizer (Pyrex). 100  $\mu$ L of brain homogenate was used for mRNA isolation  
348 with the Quiagen RNeasy Mini Kit according to manufacturer's instructions. RNA samples were  
349 stored at -80°C until ready for use.

350 *Nanostring*

351 Nanostring nCounter Mouse Immunology Max Kit was used following mRNA isolation from the  
352 brain. RNA hybridization was performed according to Nanostring manufacturer's instructions.  
353 Samples were incubated for 24 hours at 65°C and then were run on the nCounter Prep Station  
354 5s before being placed on the nCounter Digital Analyzer. The ROSALIND platform was used for  
355 data analysis.

356 *Statistical Analysis*

357 Student's unpaired t-test, One-way ANOVA, and Kaplan-Meier tests were conducted using  
358 GraphPad Prism (GraphPad Software, Inc.,)

359 *Author Contributions:* LTW and KAK conceived the studies and wrote the manuscript. LTW  
360 performed animal experiments, ELISAs, flow cytometry, RNA analysis, and data analysis. KGG  
361 assisted with animal husbandry and experiments. All authors reviewed the data and manuscript.  
362 Work was funded by T32 AI170478 (LTW), and R01 DK134366 (KAK).

363

364 Akue, A.D., Lee, J.Y., and Jameson, S.C. (2012). Derivation and maintenance of virtual memory CD8 T cells.  
365 *J Immunol* 188, 2516-2523.

366 Ashouri, J.F., and Weiss, A. (2017). Endogenous Nur77 Is a Specific Indicator of Antigen Receptor Signaling  
367 in Human T and B Cells. *J Immunol* 198, 657-668.

368 Barrios, C., Brawand, P., Berney, M., Brandt, C., Lambert, P.H., and Siegrist, C.A. (1996). Neonatal and early  
369 life immune responses to various forms of vaccine antigens qualitatively differ from adult responses:  
370 predominance of a Th2-biased pattern which persists after adult boosting. *Eur J Immunol* 26, 1489-1496.

371 Basha, S., Surendran, N., and Pichichero, M. (2014). Immune responses in neonates. *Expert Rev Clin*  
372 *Immunol* 10, 1171-1184.

373 Basu, S. (2015). Neonatal sepsis: the gut connection. *European Journal of Clinical Microbiology &*  
374 *Infectious Diseases* 34, 215-222.

375 Bergin, S.P., Thaden, J.T., Ericson, J.E., Cross, H., Messina, J., Clark, R.H., Fowler, V.G., Jr., Benjamin, D.K.,  
376 Jr., Hornik, C.P., and Smith, P.B. (2015). Neonatal Escherichia coli Bloodstream Infections: Clinical  
377 Outcomes and Impact of Initial Antibiotic Therapy. *Pediatr Infect Dis J* 34, 933-936.

378 Bizzarro, M.J., Raskind, C., Baltimore, R.S., and Gallagher, P.G. (2005). Seventy-five years of neonatal sepsis  
379 at Yale: 1928-2003. *Pediatrics* 116, 595-602.

380 Cardoso, F.L., Herz, J., Fernandes, A., Rocha, J., Sepodes, B., Brito, M.A., McGavern, D.B., and Brites, D.  
381 (2015). Systemic inflammation in early neonatal mice induces transient and lasting neurodegenerative  
382 effects. *J Neuroinflammation* 12, 82.

383 Carl, M.A., Ndao, I.M., Springman, A.C., Manning, S.D., Johnson, J.R., Johnston, B.D., Burnham, C.A.,  
384 Weinstock, E.S., Weinstock, G.M., Wylie, T.N., *et al.* (2014). Sepsis from the gut: the enteric habitat of  
385 bacteria that cause late-onset neonatal bloodstream infections. *Clin Infect Dis* 58, 1211-1218.

386 Chen, Y.S., Chen, I.B., Pham, G., Shao, T.Y., Bangar, H., Way, S.S., and Haslam, D.B. (2020). IL-17-producing  
387  $\gamma\delta$  T cells protect against Clostridium difficile infection. *J Clin Invest* 130, 2377-2390.

388 Chien, Y.-h., Meyer, C., and Bonneville, M. (2014).  $\gamma\delta$  T Cells: First Line of Defense and Beyond. *Annual*  
389 *Review of Immunology* 32, 121-155.

390 Constant, P., Davodeau, F., Peyrat, M.-A., Poquet, Y., Puzo, G., Bonneville, M., and Fournié, J.-J. (1994).  
391 Stimulation of Human  $\gamma\delta$  T Cells by Nonpeptidic Mycobacterial Ligands. *Science* 264, 267-270.

392 Cumba Garcia, L.M., Huseby Kelcher, A.M., Malo, C.S., and Johnson, A.J. (2016). Superior isolation of  
393 antigen-specific brain infiltrating T cells using manual homogenization technique. *J Immunol Methods*  
394 439, 23-28.

395 Dimova, T., Brouwer, M., Gosselin, F., Tassignon, J., Leo, O., Donner, C., Marchant, A., and Vermijlen, D.  
396 (2015). Effector  $\gamma\delta$  T cells dominate the human fetal  $\gamma\delta$  T-cell repertoire. *Proc Natl Acad Sci U S A*  
397 112, E556-565.

398 Doebele, R.C., Busch, R., Scott, H.M., Pashine, A., and Mellins, E.D. (2000). Determination of the HLA-DM  
399 interaction site on HLA-DR molecules. *Immunity* 13, 517-527.

400 Dong, Y., and Speer, C.P. (2015). Late-onset neonatal sepsis: recent developments. *Archives of disease in*  
401 *childhood Fetal and neonatal edition* 100, F257-F263.

402 Doran, K.S., Engelson, E.J., Khosravi, A., Maisey, H.C., Fedtke, I., Equils, O., Michelsen, K.S., Ardit, M.,  
403 Peschel, A., and Nizet, V. (2005). Blood-brain barrier invasion by group B Streptococcus depends upon  
404 proper cell-surface anchoring of lipoteichoic acid. *The Journal of Clinical Investigation* 115, 2499-2507.

405 Gelderblom, M., Arunachalam, P., and Magnus, T. (2014).  $\gamma\delta$  T cells as early sensors of tissue damage and  
406 mediators of secondary neurodegeneration. *Front Cell Neurosci* 8, 368.

407 Gentles, A.J., Newman, A.M., Liu, C.L., Bratman, S.V., Feng, W., Kim, D., Nair, V.S., Xu, Y., Khuong, A.,  
408 Hoang, C.D., *et al.* (2015). The prognostic landscape of genes and infiltrating immune cells across human  
409 cancers. *Nat Med* 21, 938-945.

410 Gibbons, D.L., Haque, S.F., Silberzahn, T., Hamilton, K., Langford, C., Ellis, P., Carr, R., and Hayday, A.C.  
411 (2009). Neonates harbour highly active gammadelta T cells with selective impairments in preterm infants.  
412 *Eur J Immunol* 39, 1794-1806.

413 Guo, X.J., Dash, P., Crawford, J.C., Allen, E.K., Zamora, A.E., Boyd, D.F., Duan, S., Bajracharya, R., Awad,  
414 W.A., Apiwattanakul, N., *et al.* (2018). Lung  $\gamma\delta$  T Cells Mediate Protective Responses during Neonatal  
415 Influenza Infection that Are Associated with Type 2 Immunity. *Immunity* 49, 531-544.e536.

416 Haas, J.D., González, F.H.M., Schmitz, S., Chennupati, V., Föhse, L., Kremmer, E., Förster, R., and Prinz, I.  
417 (2009). CCR6 and NK1.1 distinguish between IL-17A and IFN- $\gamma$ -producing  $\gamma\delta$  effector T cells. *European  
418 Journal of Immunology* 39, 3488-3497.

419 Haluszczak, C., Akue, A.D., Hamilton, S.E., Johnson, L.D., Pujanauski, L., Teodorovic, L., Jameson, S.C., and  
420 Kedl, R.M. (2009). The antigen-specific CD8+ T cell repertoire in unimmunized mice includes memory  
421 phenotype cells bearing markers of homeostatic expansion. *J Exp Med* 206, 435-448.

422 Harris, T.O., Shelver, D.W., Bohnsack, J.F., and Rubens, C.E. (2003). A novel streptococcal surface protease  
423 promotes virulence, resistance to opsonophagocytosis, and cleavage of human fibrinogen. *The Journal of  
424 Clinical Investigation* 111, 61-70.

425 Heath, P.T., and Jardine, L.A. (2014). Neonatal infections: group B streptococcus. *BMJ Clin Evid* 2014.

426 Hoffman, J.A., Wass, C., Stins, M.F., and Kim, K.S. (1999). The capsule supports survival but not traversal  
427 of *Escherichia coli* K1 across the blood-brain barrier. *Infect Immun* 67, 3566-3570.

428 Kaczmarek, A., Budzyńska, A., and Gospodarek, E. (2014). Detection of K1 antigen of *Escherichia coli* rods  
429 isolated from pregnant women and neonates. *Folia Microbiol (Praha)* 59, 419-422.

430 Kambayashi, T., and Laufer, T.M. (2014). Atypical MHC class II-expressing antigen-presenting cells: can  
431 anything replace a dendritic cell? *Nat Rev Immunol* 14, 719-730.

432 Kim, K.S. (2006). Meningitis-Associated <i>Escherichia coli</i>. *EcoSal Plus* 2,  
433 10.1128/ecosalplus.1128.1126.1121.1122.

434 Knoop, K.A., Coughlin, P.E., Floyd, A.N., Ndao, I.M., Hall-Moore, C., Shaikh, N., Gasparrini, A.J., Rusconi, B.,  
435 Escobedo, M., Good, M., *et al.* (2020). Maternal activation of the EGFR prevents translocation of gut-  
436 residing pathogenic *Escherichia coli* in a model of late-onset neonatal sepsis. *Proceedings of the National  
437 Academy of Sciences of the United States of America* 117, 7941-7949.

438 Lee, J.Y., Hamilton, S.E., Akue, A.D., Hogquist, K.A., and Jameson, S.C. (2013). Virtual memory CD8 T cells  
439 display unique functional properties. *Proc Natl Acad Sci U S A* 110, 13498-13503.

440 Li, L., Lee, H.H., Bell, J.J., Gregg, R.K., Ellis, J.S., Gessner, A., and Zaghouani, H. (2004). IL-4 utilizes an  
441 alternative receptor to drive apoptosis of Th1 cells and skews neonatal immunity toward Th2. *Immunity*  
442 20, 429-440.

443 Moran, A.E., Holzapfel, K.L., Xing, Y., Cunningham, N.R., Maltzman, J.S., Punt, J., and Hogquist, K.A. (2011).  
444 T cell receptor signal strength in Treg and iNKT cell development demonstrated by a novel fluorescent  
445 reporter mouse. *J Exp Med* 208, 1279-1289.

446 Muñoz-Ruiz, M., Sumaria, N., Pennington, D.J., and Silva-Santos, B. (2017). Thymic Determinants of  $\gamma\delta$  T  
447 Cell Differentiation. *Trends Immunol* 38, 336-344.

448 Mynarek, M., Bjellmo, S., Lydersen, S., Afset, J.E., Andersen, G.L., and Vik, T. (2021). Incidence of invasive  
449 Group B Streptococcal infection and the risk of infant death and cerebral palsy: a Norwegian Cohort Study.  
450 *Pediatr Res* 89, 1541-1548.

451 Nam, J.S., Terabe, M., Kang, M.J., Chae, H., Voong, N., Yang, Y.A., Laurence, A., Michalowska, A., Mamura,  
452 M., Lonning, S., *et al.* (2008). Transforming growth factor beta subverts the immune system into directly  
453 promoting tumor growth through interleukin-17. *Cancer Res* 68, 3915-3923.

454 Park, J.H., Kang, I., and Lee, H.K. (2022).  $\gamma\delta$  T Cells in Brain Homeostasis and Diseases. *Front Immunol* 13,  
455 886397.

456 Remington, J.S., Wilson, C.B., Nizet, V., Klein, J.O., and Maldonado, Y. (2010). Infectious diseases of the  
457 fetus and newborn E-book (Elsevier Health Sciences).

458 Ribeiro, M., Brigas, H.C., Temido-Ferreira, M., Pousinha, P.A., Regen, T., Santa, C., Coelho, J.E., Marques-  
459 Morgado, I., Valente, C.A., Omenetti, S., *et al.* (2019a). Meningeal  $\gamma\delta$  T cell-derived IL-17 controls synaptic  
460 plasticity and short-term memory. *Sci Immunol* 4.

461 Ribeiro, M., Brigas, H.C., Temido-Ferreira, M., Pousinha, P.A., Regen, T., Santa, C., Coelho, J.E., Marques-  
462 Morgado, I., Valente, C.A., Omenetti, S., *et al.* (2019b). Meningeal  $\gamma\delta$  T cell-derived IL-17 controls synaptic  
463 plasticity and short-term memory. *Science Immunology* 4, eaay5199.

464 Ribot, J.C., deBarros, A., Pang, D.J., Neves, J.F., Peperzak, V., Roberts, S.J., Girardi, M., Borst, J., Hayday,  
465 A.C., Pennington, D.J., *et al.* (2009). CD27 is a thymic determinant of the balance between interferon-  
466 gamma- and interleukin 17-producing gammadelta T cell subsets. *Nat Immunol* 10, 427-436.

467 Ribot, J.C., Lopes, N., and Silva-Santos, B. (2021).  $\gamma\delta$  T cells in tissue physiology and surveillance. *Nature*  
468 *Reviews Immunology* 21, 221-232.

469 Santambrogio, L., Berendam, S.J., and Engelhard, V.H. (2019). The Antigen Processing and Presentation  
470 Machinery in Lymphatic Endothelial Cells. *Front Immunol* 10, 1033.

471 Schüler, T., Hämerling, G.n.J., and Arnold, B. (2004). Cutting Edge: IL-7-Dependent Homeostatic  
472 Proliferation of CD8+ T Cells in Neonatal Mice Allows the Generation of Long-Lived Natural Memory T Cells  
473 1. *The Journal of Immunology* 172, 15-19.

474 Sedlak, C., Patzl, M., Saalmüller, A., and Gerner, W. (2014). IL-12 and IL-18 induce interferon- $\gamma$  production  
475 and de novo CD2 expression in porcine  $\gamma\delta$  T cells. *Dev Comp Immunol* 47, 115-122.

476 Segura-Cervantes, E., Mancilla-Ramírez, J., González-Canudas, J., Alba, E., Santillán-Ballesteros, R.,  
477 Morales-Barquet, D., Sandoval-Plata, G., and Galindo-Sevilla, N. (2016). Inflammatory Response in  
478 Preterm and Very Preterm Newborns with Sepsis. *Mediators Inflamm* 2016, 6740827.

479 Semmes, E.C., Chen, J.-L., Goswami, R., Burt, T.D., Permar, S.R., and Fouda, G.G. (2021). Understanding  
480 Early-Life Adaptive Immunity to Guide Interventions for Pediatric Health. *Frontiers in Immunology* 11.

481 Silva-Santos, B., Mensurado, S., and Coffelt, S.B. (2019).  $\gamma\delta$  T cells: pleiotropic immune effectors with  
482 therapeutic potential in cancer. *Nat Rev Cancer* 19, 392-404.

483 Stoll, B.J., Hansen, N.I., Adams-Chapman, I., Fanaroff, A.A., Hintz, S.R., Vohr, B., Higgins, R.D., National  
484 Institute of Child, H., and Human Development Neonatal Research Network, f.t. (2004).  
485 Neurodevelopmental and Growth Impairment Among Extremely Low-Birth-Weight Infants With Neonatal  
486 Infection. *JAMA* 292, 2357-2365.

487 Stoll, B.J., Hansen, N.I., Sánchez, P.J., Faix, R.G., Poindexter, B.B., Van Meurs, K.P., Bizzarro, M.J., Goldberg,  
488 R.N., Frantz, I.D., 3rd, Hale, E.C., *et al.* (2011). Early onset neonatal sepsis: the burden of group B  
489 Streptococcal and *E. coli* disease continues. *Pediatrics* 127, 817-826.

490 Tavares, T., Pinho, L., and Bonifácio Andrade, E. (2022). Group B Streptococcal Neonatal Meningitis. *Clin*  
491 *Microbiol Rev* 35, e0007921.

492 Tsafaras, G.P., Ntontsi, P., and Xanthou, G. (2020). Advantages and Limitations of the Neonatal Immune  
493 System. *Front Pediatr* 8.

494 Tsai, M.H., Hsu, J.F., Chu, S.M., Lien, R., Huang, H.R., Chiang, M.C., Fu, R.H., Lee, C.W., and Huang, Y.C.  
495 (2014). Incidence, clinical characteristics and risk factors for adverse outcome in neonates with late-onset  
496 sepsis. *Pediatr Infect Dis J* 33, e7-e13.

497 Vantourout, P., and Hayday, A. (2013). Six-of-the-best: unique contributions of  $\gamma\delta$  T cells to immunology.  
498 *Nature Reviews Immunology* 13, 88-100.

499 Welte, T., Lamb, J., Anderson, J.F., Born, W.K., O'Brien, R.L., and Wang, T. (2008). Role of two distinct  
500 gammadelta T cell subsets during West Nile virus infection. *FEMS Immunol Med Microbiol* 53, 275-283.

501 Wijdeven, R.H., van Luijn, M.M., Wierenga-Wolf, A.F., Akkermans, J.J., van den Elsen, P.J., Hintzen, R.Q.,  
502 and Neefjes, J. (2018). Chemical and genetic control of IFNy-induced MHCII expression. *EMBO Rep* 19.

503 Wo, J., Zhang, F., Li, Z., Sun, C., Zhang, W., and Sun, G. (2020). The Role of Gamma-Delta T Cells in Diseases  
504 of the Central Nervous System. *Frontiers in Immunology* 11.

505 Wynn, J.L., Guthrie, S.O., Wong, H.R., Lahni, P., Ungaro, R., Lopez, M.C., Baker, H.V., and Moldawer, L.L.  
506 (2015). Postnatal Age Is a Critical Determinant of the Neonatal Host Response to Sepsis. *Mol Med* 21, 496-  
507 504.  
508 Wynn, J.L., Wilson, C.S., Hawiger, J., Scumpia, P.O., Marshall, A.F., Liu, J.H., Zharkikh, I., Wong, H.R., Lahni,  
509 P., Benjamin, J.T., *et al.* (2016). Targeting IL-17A attenuates neonatal sepsis mortality induced by IL-18.  
510 *Proc Natl Acad Sci U S A* 113, E2627-2635.  
511 Xu, S., and Cao, X. (2010). Interleukin-17 and its expanding biological functions. *Cell Mol Immunol* 7, 164-  
512 174.

513

514

**Figure 1:  $\gamma\delta$  T cells Respond to *E. coli* and GBS Neonatal Sepsis and Differentially Drive Mortality**

A) Gating scheme (L) and quantification (R) of CD69+, CD62L- splenic  $\gamma\delta$ + T cells in postnatal day 7 (P7) 18 hours post-infection with either  $2 \times 10^4$  CFU *E. coli* or  $10^6$  CFU GBS COH-1 B) Survival curves of BL/6 P7 pups infected with *E. coli* or C) GBS treated with either isotype IgG or 15  $\mu$ g/g anti-TCR $\gamma\delta$  antibody D) Bacterial CFUs from the livers of GBS and *E. coli* infected pups treated with anti-TCR $\gamma\delta$  antibody. Data shown is from four independent experiments, n>3 mice per group. Statistical tests used include one-way ANOVA (A, D), and Kaplan-Meier (B, C). with ns p>0.5

**Figure 2: *E. coli* and GBS Neonatal Sepsis Drive Distinct Effector Cytokine Responses from  $\gamma\delta$  T cells**

A) Flow cytometry gating scheme of IFN- $\gamma$ + and IL-17+ splenic  $\gamma\delta$ + T cells from uninfected, GBS, and *E. coli* infected BL/6 P7 pups. B) Mean fluorescent intensity (MFI) of IFN- $\gamma$  and C) IL-17 from splenic  $\gamma\delta$ + T cells 18 hours post-infection. D) IFN- $\gamma$  and E) IL-17 serum ELISA. F) Proportion of activated CD27+ and G) CCR6+  $\gamma\delta$ + T cells from uninfected, GBS, and *E. coli* infected BL/6 P7 pups. Data shown is from three independent experiments, n>3 mice per group, statistical tests used include one-way ANOVA with ns p>0.5.

**Figure 3: Neuroinflammation is a Feature of *E. coli* and GBS Neonatal Sepsis**

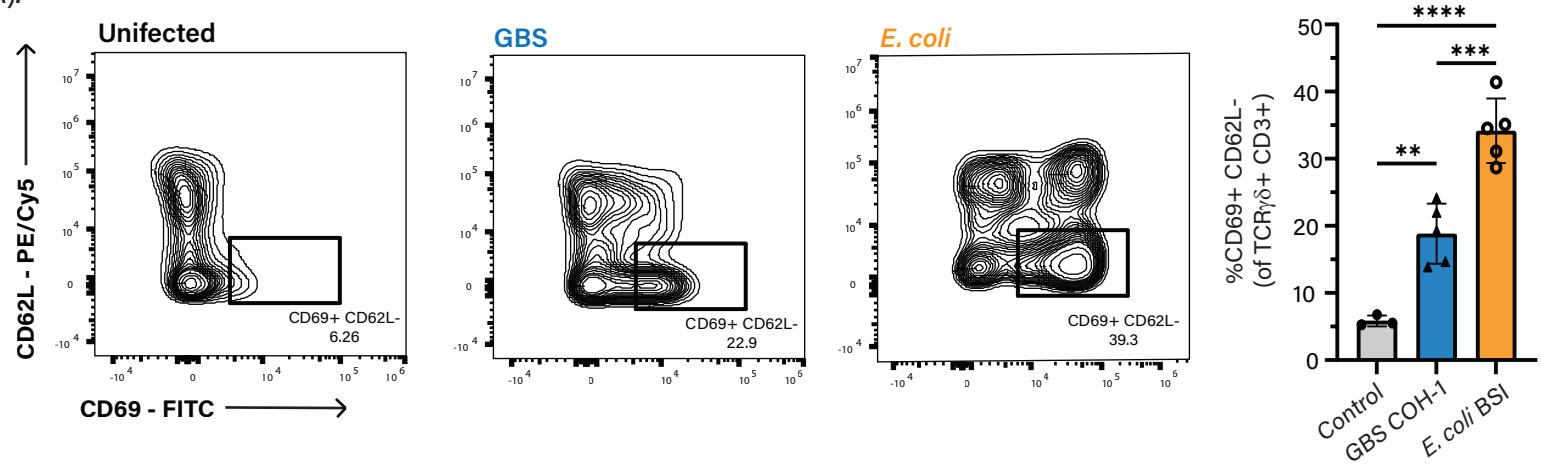
A) GBS and *E. coli* CFUs from the brains of BL/6 P7 pups B) Absolute number of monocytes (CD45hi, CD11b+, Ly6C+, Ly6G-) and C) Neutrophils (CD45hi, CD11b+, Ly6C-, Ly6G+) in the perfused brains of *E. coli* and GBS infected BL/6 P7 pups 18 hours post-infection. D) Volcano plot of differentially expressed genes between BL/6 uninfected control vs. *E. coli* infected P7 pups and E) GBS infected P7 pups. Data shown is from four independent experiments, n>4 mice per group. Statistical tests used include Student's unpaired t-test (A), one-way ANOVA (B,C) with ns p>0.5.

**Figure 4: TCR-Specific Activation of  $\gamma\delta$ + T cells Occurs During *E. coli*, but not GBS, Septicemia and Differentially Drives Neuroinflammation**

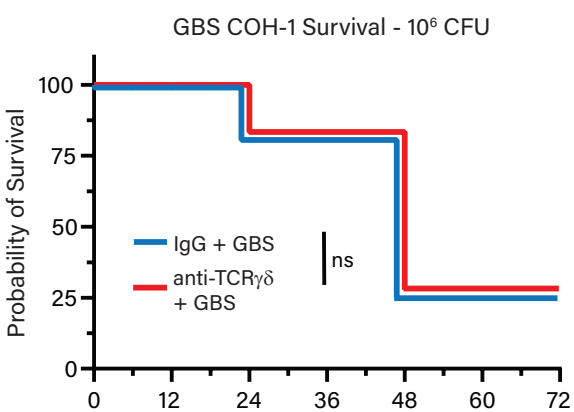
Proportion of Nur77+ CD69+  $\gamma\delta$ + T cells in the A) Spleen and B) Brain of GBS and *E. coli* infected Nur77-GFP P7 pups. C) CCR6 expression of Nur77+ CD69+  $\gamma\delta$ + T cells in the spleen and brain of *E. coli*-infected pups. D) Volcano plots of differentially expressed genes in the brains of *E. coli* infected, or E) GBS-infected BL/6 vs. TCR $\delta$ -/- P7 pups. Data shown is from three independent experiments, n>3 mice per group. Statistics used include one-way ANOVA (A,B) with ns p>0.5.

## Fig. 1: $\gamma\delta$ T cells Respond to *E. coli* and GBS Neonatal Sepsis and Differentially Contribute to Mortality

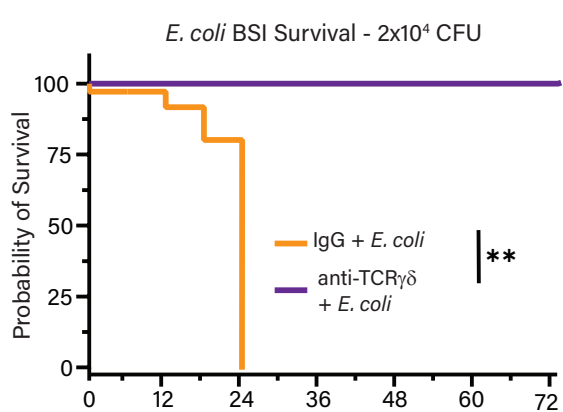
A).



B).



C).



D).

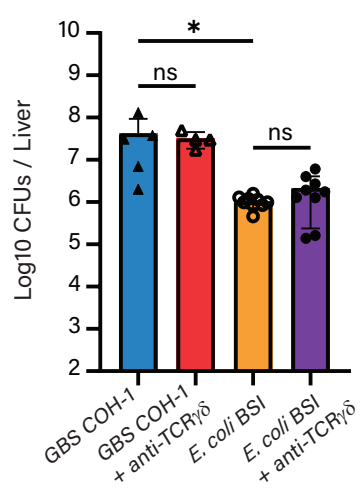
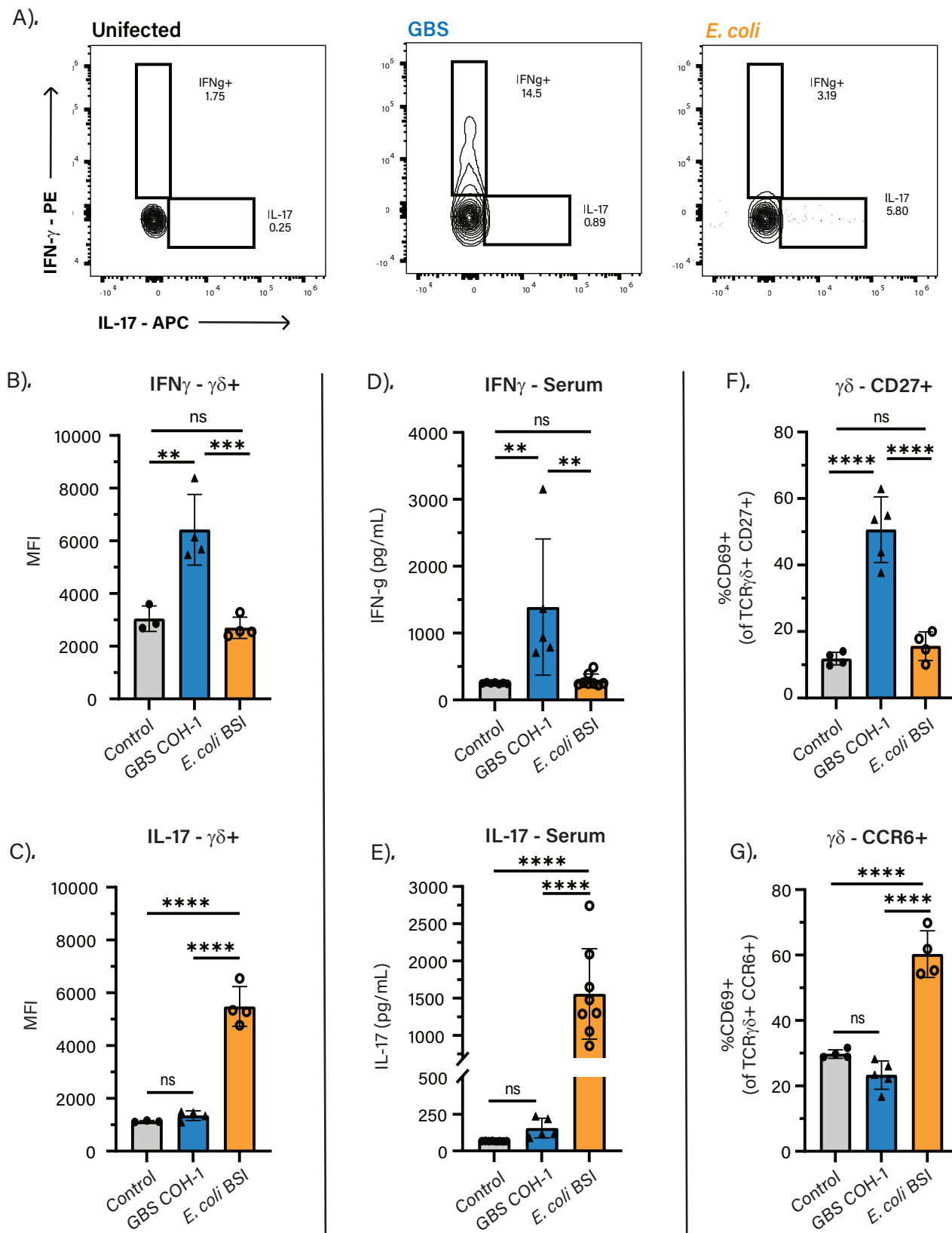


Fig. 2: *E. coli* and GBS Neonatal Sepsis Drive Distinct Effector Cytokine Responses from  $\gamma\delta$  T cells



**Fig. 3. Neuroinflammation is a feature of GBS and *E. coli* Meningoencephalitis**

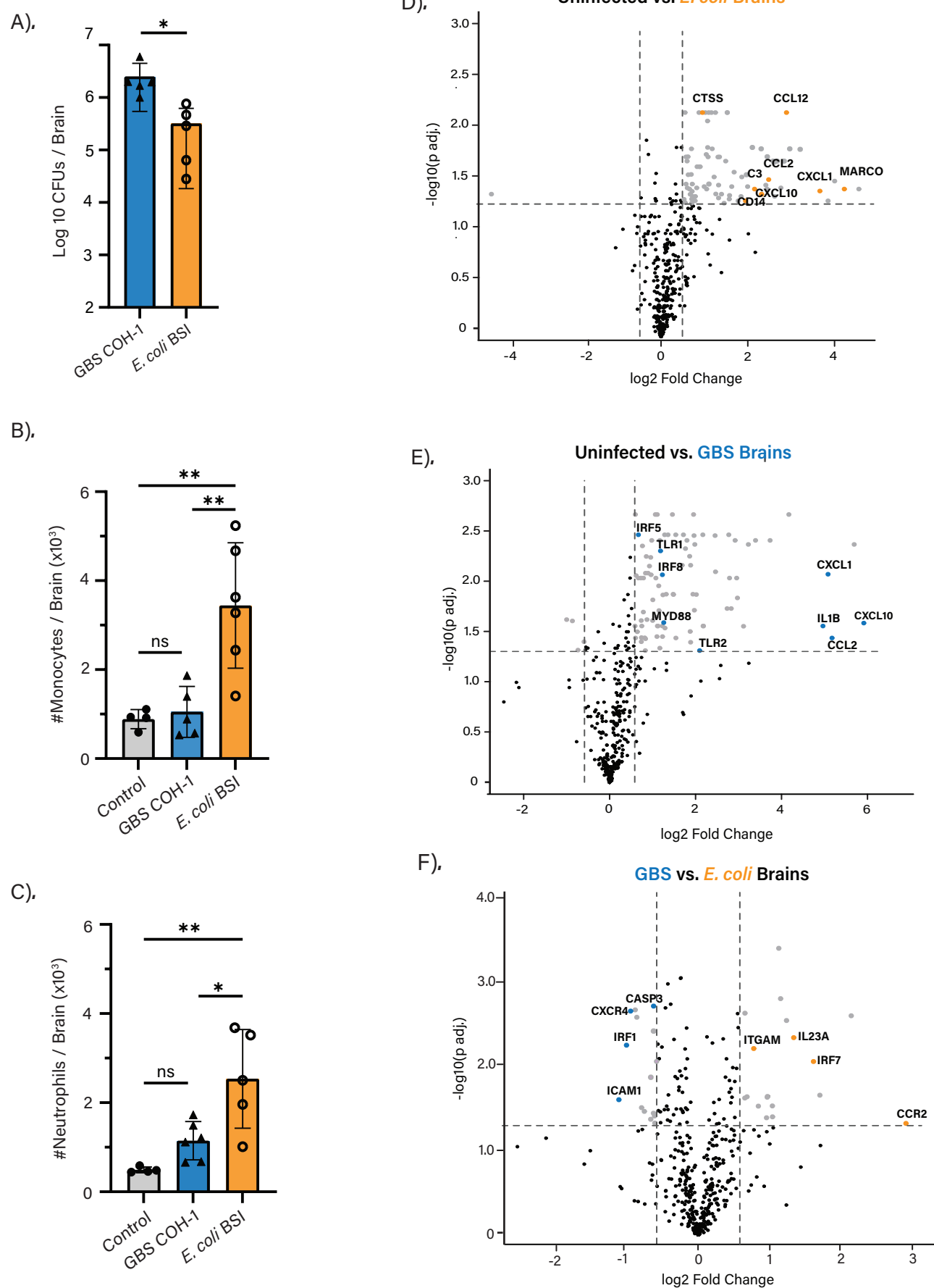
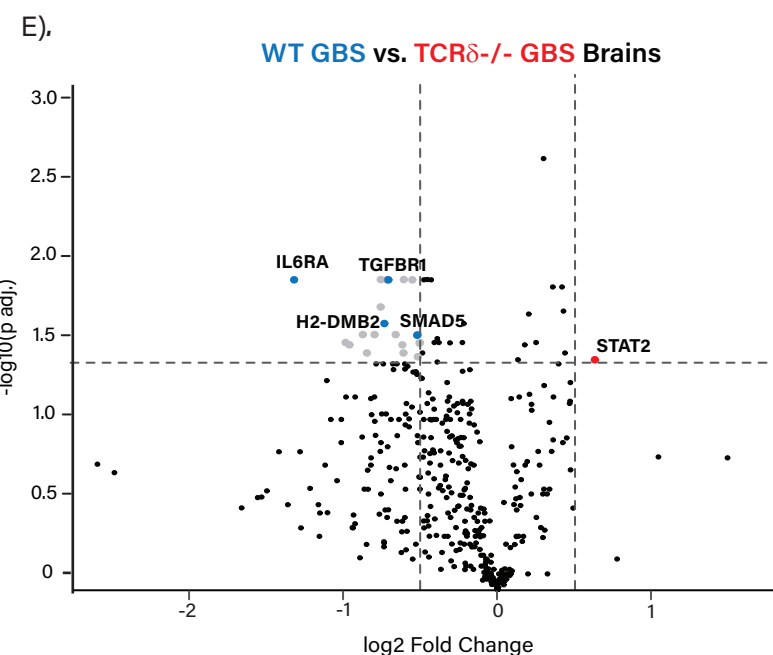
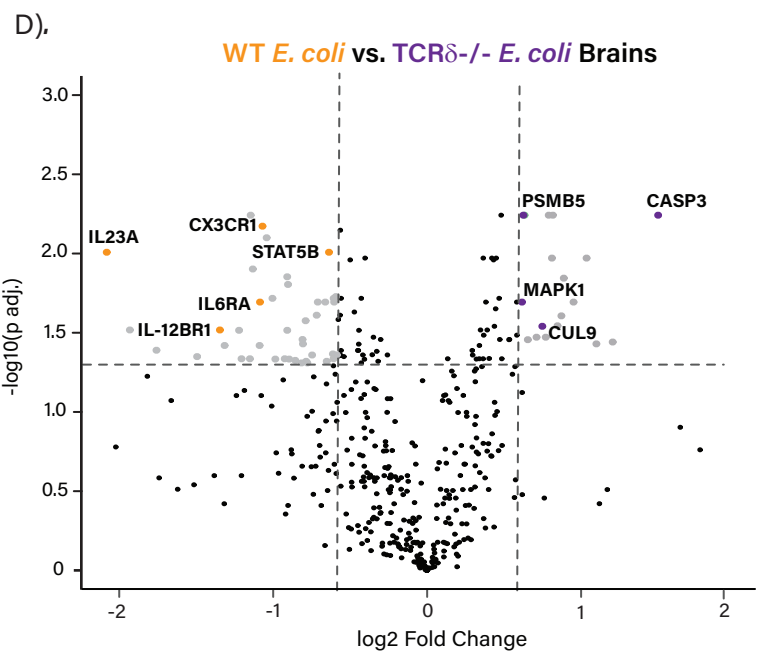
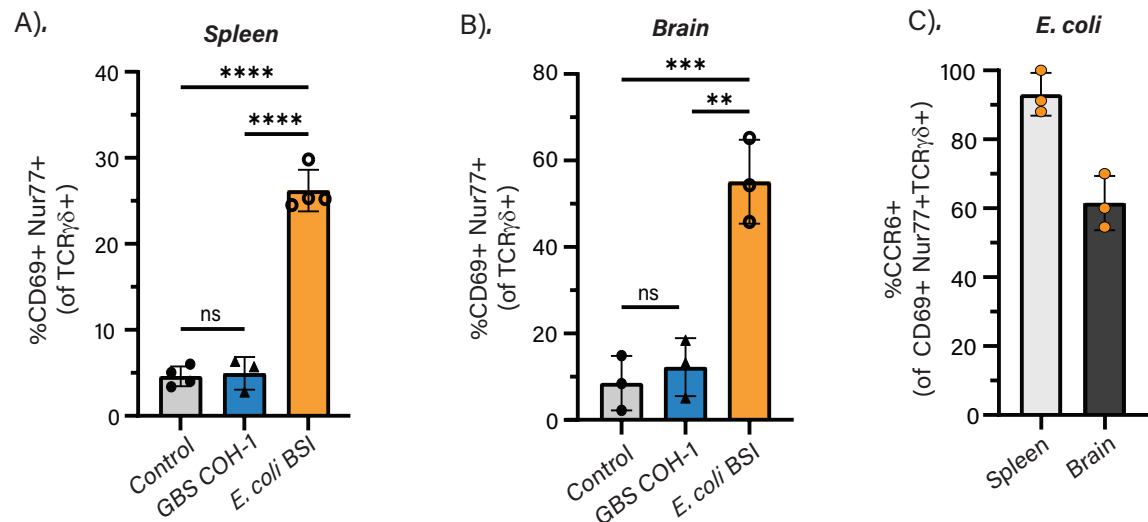


Fig. 4: TCR-Specific Activation of  $\gamma\delta$  T Cells Occurs During *E. coli*, but not GBS, Septicemia and Differentially Drives Neuroinflammation



**Figure S1: Responses of CD4+ and CD8+ T Cells, and B cells to GBS and *E. coli* Neonatal Sepsis**

A) Flow cytometric staining of CD69+, CD62L- splenic CD4, B) CD8 T cells and C) B cells 18 hours-post *E. coli* or GBS infection in P7 BL/6 pups. Data shown is from two independent experiments, n>3 mice per group, statistical tests used include one-way ANOVA, ns p>0.5.

**Figure S2: Flow Cytometry Gating Scheme of Neonatal Brain Immune Cell Populations**

A) Live, single cells in the brain were gated on CD45, with CD45mid population representing microglia (CD11b+, CX3CR1+). The CD45hi compartment was gated into TCR $\gamma\delta$ + or CD11b+. CD11b+ cells were then gated into Ly6C+, Ly6G- (Monocytes), or Ly6C-, Ly6G+ (Neutrophils).

**Figure S3: Lack of Depletion of Brain-Resident T Cells Upon Systemic anti-TCR $\gamma\delta$  Antibody Administration**

A) Absolute number of  $\gamma\delta$ + T cells in the spleen and B) brain of BL/6 P7 pups intraperitoneally injected with 15  $\mu$ g/g anti-TCR $\gamma\delta$  antibody (clone: UC7-13D5). Data shown is from two independent experiments, n>4 mice per group. Statistical tests used include Student's unpaired t-test (A,B), with ns p>0.5.